INAUGURAL ARTICLE

PLANT BIOLOGY

Spatial and temporal regulation of biosynthesis of the plant immune signal salicylic acid

Xiao-yu Zheng[a,b,1,2], Mian Zhou[a,b,1,3], Heejin Yoo[a,b,1], Jose L. Pruneda-Paz[c,d], Natalie Weaver Spivey[a,b,4], Steve A. Kay[d,e], and Xinnian Dong[a,b,5]

[a]Howard Hughes Medical Institute-Gordon and Betty Moore Foundation, Duke University, Durham, NC 27708; [b]Department of Biology, Duke University, Durham, NC 27708; [c]Division of Biological Sciences, University of California, San Diego, La Jolla, CA 92093; [d]Center for Chronobiology, University of California, San Diego, La Jolla, CA 92093; and [e]Molecular and Computational Biology Section, University of Southern California, Los Angeles, CA 90089

This contribution is part of the special series of Inaugural Articles by members of the National Academy of Sciences elected in 2012.

Contributed by Xinnian Dong, June 8, 2015 (sent for review April 1, 2015; reviewed by Jean T. Greenberg)

The plant hormone salicylic acid (SA) is essential for local defense and systemic acquired resistance (SAR). When plants, such as *Arabidopsis*, are challenged by different pathogens, an increase in SA biosynthesis generally occurs through transcriptional induction of the key synthetic enzyme isochorismate synthase 1 (ICS1). However, the regulatory mechanism for this induction is poorly understood. Using a yeast one-hybrid screen, we identified two transcription factors (TFs), NTM1-LIKE 9 (NTL9) and CCA1 HIKING EXPEDITION (CHE), as activators of *ICS1* during specific immune responses. NTL9 is essential for inducing *ICS1* and two other SA synthesis-related genes, *PHYTOALEXIN-DEFICIENT 4* (*PAD4*) and *ENHANCED DISEASE SUSCEPTIBILITY 1* (*EDS1*), in guard cells that form stomata. Stomata can quickly close upon challenge to block pathogen entry. This stomatal immunity requires *ICS1* and the SA signaling pathway. In the *ntl9* mutant, this response is defective and can be rescued by exogenous application of SA, indicating that NTL9-mediated SA synthesis is essential for stomatal immunity. CHE, the second identified TF, is a central circadian clock oscillator and is required not only for the daily oscillation in SA levels but also for the pathogen-induced SA synthesis in systemic tissues during SAR. CHE may also regulate *ICS1* through the known transcription activators CALMODULIN BINDING PROTEIN 60g (CBP60g) and SYSTEMIC ACQUIRED RESISTANCE DEFICIENT 1 (SARD1) because induction of these TF genes is compromised in the *che-2* mutant. Our study shows that SA biosynthesis is regulated by multiple TFs in a spatial and temporal manner and therefore fills a gap in the signal transduction pathway between pathogen recognition and SA production.

plant immunity | transcription regulation | circadian clock | systemic acquired resistance | stomatal immunity

Salicylic acid (SA) is a plant defense hormone required for both local defense and systemic acquired resistance (SAR) (1, 2). For some plants, such as tobacco and *Arabidopsis*, SA biosynthesis is significantly induced upon challenge by a wide range of pathogens, such as tobacco mosaic virus and the bacterial phytopathogen *Pseudomonas syringae* (3, 4). An increase in the endogenous SA level and exogenous application of SA can both lead to broad-spectrum disease resistance (3–5). For these plants, blocking SA accumulation significantly compromises the plants' ability to combat biotrophic pathogens (6, 7). In other plants with high basal SA levels, like rice and potato, even though SA is not induced by pathogen infection, depletion of endogenous SA in these plants also significantly reduces their resistance against pathogens (8, 9). Because SA can induce massive production of antimicrobial pathogenesis-related (PR) proteins and the plant secretory pathway for their proper folding and transport, it is believed that SA promotes plant immunity against a broad spectrum of pathogens through the combined activities of these antimicrobial proteins (3, 10, 11). More recently, SA was shown to play a role in stomatal immunity, which involves perception of bacterial flagellin by the host receptor FLAGELLIN-SENSING 2 (FLS2) and the subsequent closure of stomata to block entry of bacterial pathogens into plants (12, 13). Both the SA synthesis mutant isochorismate synthase 1 (*ics1*) and the SA signaling mutant nonexpresser of *PR* genes 1 (*npr1*) are defective in stomatal immunity (12, 13).

Pathogen-induced SA synthesis mainly occurs in the chloroplast via the activity of ICS1 (14, 15). Correlating with the increase in SA levels, expression of *ICS1* is induced both locally and systemically (14). Therefore, it is hypothesized that the transcriptional regulation of *ICS1* is a key step in activating defense responses in plants such as tobacco and *Arabidopsis*. Several transcription factors (TFs) have been identified for their direct binding activities to the promoter of *ICS1* and regulation of its expression (16–19). Most of these TFs, such as EIN3 (ETHYLENE-INSENSITIVE 3) and ANAC019 (*Arabidopsis* NAC domain-containing protein 19), are negative regulators of *ICS1* and SA levels and may function in the cross-talk between different plant hormones necessary for fine-tuning growth and defense (16, 17). So far, two closely-related TFs, SARD1 (SYSTEMIC ACQUIRED RESISTANCE DEFICIENT 1) and CBP60g

Significance

Biosynthesis of the plant immune signal salicylic acid (SA) is normally induced upon pathogen challenge through transcriptional activation of the key SA synthetic enzyme gene, *ICS1*. However, how different pathogenic signals trigger SA synthesis in both local and systemic tissues and during different immune responses is poorly understood. Our study filled this knowledge gap by the identification of two transcription factors (TFs): one is required for SA biosynthesis in stomata to prevent pathogen entry through these epidermal openings, and the other is essential for both the circadian oscillation in SA levels and the accumulation of SA in distal tissue during systemic acquired resistance. Our study shows that SA biosynthesis is regulated by multiple TFs in a spatial and temporal manner.

Author contributions: X.-y.Z., M.Z., H.Y., N.W.S., and X.D. designed research; X.-y.Z., M.Z., H.Y., J.L.P.-P., and N.W.S. performed research; J.L.P.-P. and S.A.K. contributed new reagents/analytic tools; X.-y.Z., M.Z., and H.Y. analyzed data; and X.-y.Z., M.Z., and X.D. wrote the paper.

Reviewers included: J.T.G., University of Chicago.

The authors declare no conflict of interest.

Freely available online through the PNAS open access option.

[1]X.-y.Z., M.Z., and H.Y. contributed equally to this work.

[2]Present address: Howard Hughes Medical Institute, Department of Molecular and Cellular Biology, FAS Center for Systems Biology, Harvard University, Cambridge, MA 02138.

[3]Present address: Department of Plant Pathology and Microbiology, Iowa State University, Ames, IA 50011.

[4]Present address: Department of Biology, Wofford College, Spartanburg, SC 29303.

[5]To whom correspondence should be addressed. Email: xdong@duke.edu.

This article contains supporting information online at www.pnas.org/lookup/suppl/doi:10.1073/pnas.1511182112/-/DCSupplemental.

(CALMODULIN BINDING PROTEIN 60g), and TCP (TEOSINTE BRANCHED1, CYCLOIDEA, and PCF) family TFs TCP8 and TCP9 have been identified as positive regulators required for *ICS1* induction and SA accumulation upon pathogen infection (18, 20, 21).

Despite the discoveries of these SA-regulating TFs, many important questions remain to be answered. Because SA-mediated responses are spatially different (e.g., local and systemic), are there tissue-specific or even cell type-specific regulators of SA synthesis? Recently, total SA content (i.e., free SA and conjugated forms) was reported to oscillate in a circadian rhythm (22), allowing plants to anticipate pathogen attack at a specific time of the day (23). This phenomenon indicates that SA synthesis may also be temporally regulated. To address these questions, we screened for *Arabidopsis* TFs that bind to the promoter of *ICS1* and found NTM1-LIKE 9 (NTL9) (TAIR number AT4G35580) (24) and CCA1 HIKING EXPEDITION (CHE) (TAIR number AT5G08330) (25), which activate *ICS1* in different immune mechanisms. NTL9 is responsible for the flagellin-induced *ICS1* expression in guard cells and stomatal immunity whereas CHE regulates the circadian oscillation of *ICS1* and SA level, as well as systemic induction of *ICS1* and SA synthesis during SAR. Our study demonstrates that SA biosynthesis is regulated by multiple TFs with temporal and spatial specificities.

Results

Identification of NTL9 and CHE as TFs Binding to the Promoter of the SA Synthesis Gene *ICS1*. To identify TFs that regulate the expression of *ICS1* and SA biosynthesis, we used the yeast one-hybrid system to screen a genome-wide collection of *Arabidopsis* TFs (26) with the promoter of *ICS1* as bait. After the initial screen and a second round of individual tests, we identified 16 candidate TFs showing greater than threefold induction in reporter activities compared with the empty vector control (Dataset S1).

In addition to *ICS1*, there are several other genes known to be required for SA accumulation (27–29). Among them, *ENHANCED DISEASE SUSCEPTIBILITY 1* (*EDS1*), *PHYTOALEXIN-DEFICIENT 4* (*PAD4*), and *avrPphB SUSCEPTIBLE 3* (*PBS3*) were coordinately regulated with *ICS1* in a microarray dataset (NASCARRAYS-168) generated from an infection time course by *P. syringae* (Dataset S2). Based on the hypothesis that these genes are coregulated, we examined candidate TFs for binding to the promoters of *EDS1, PAD4*, and *PBS3* using the same yeast one-hybrid system. Among the 16 candidates, TCP14, TCP19, NTL9, and BETA-AMYLASE 2 (BMY2) were confirmed to bind to all of the promoters tested (Fig. 1 *A* and *B* and Fig. S1). The functionalities of these four TFs were then tested in planta by infiltrating the individual TF mutants with *Pseudomonas syringae* pv. *maculicola* (*Psm*) ES4326. We found no consistent difference in *ICS1, PBS3, PAD4*, and *EDS1* gene induction or pathogen growth and disease symptom development between these mutants and the WT plants.

To help further specify possible roles of the 16 candidate TF genes in different defense responses, we examined their spatial and temporal expression profiles according to the publicly available microarray data (30, 31). We made two interesting findings: First, *NTL9* is a TF gene whose expression is much higher in guard cells than mesophyll cells (Fig. S2 and Dataset S1) (32). Because SA signaling is required for stomatal immunity (12, 13), the guard cell-preferential expression pattern of *NTL9* suggests that it might regulate SA level and immunity in this specific cell type. Second, CHE (32), a central circadian clock component, not only binds to the promoter of *ICS1* (Fig. 1*A*) but also has a circadian expression pattern in-phase with *ICS1* (33), suggesting that it might play a role in the temporal regulation of *ICS1* expression and SA synthesis.

NTL9 has been studied previously for its function in leaf senescence and immunity (34–37). By examining transgenic plants

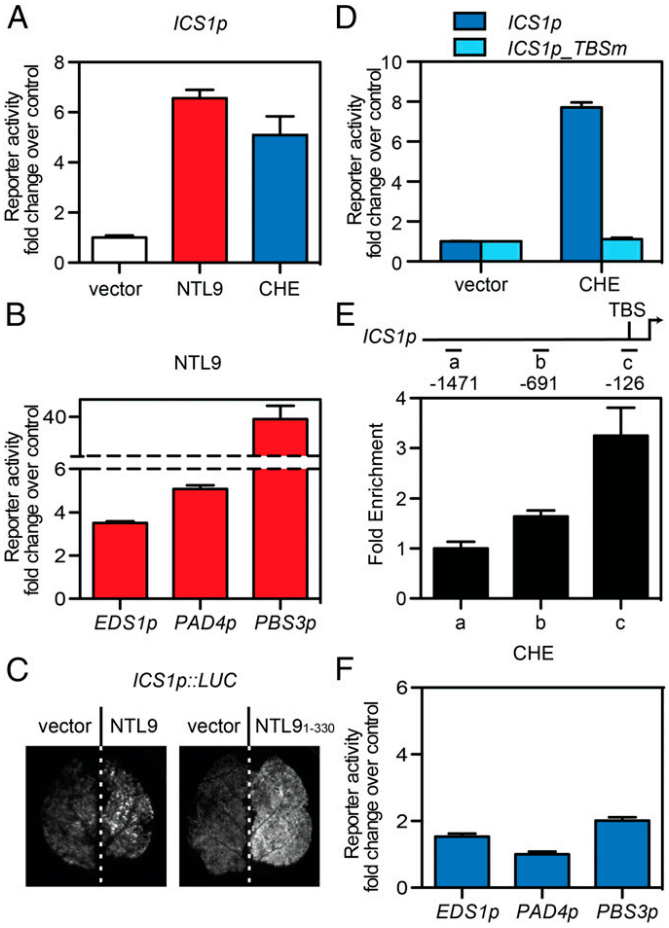

Fig. 1. CHE and NTL9 both interact with the promoter of *ICS1*. (*A, B, D*, and *F*) β-galactosidase reporter activities are shown as fold change over the empty AD (Gal4 activation domain) vector control (i.e., without the TF fusion) in Y1H strains with (*A*) *ICS1* promoter and CHE-AD or NTL9-AD; (*B*) *EDS1, PAD4*, or *PBS3* promoter and NTL9-AD; (*D*) *ICS1* or *ICS1-TBSm* promoter and CHE-AD; (*F*) *EDS1, PAD4*, or *PBS3* promoter and CHE-AD. In *A, B, E*, and *F*, error bars represent SD from three replicates. (*C*) Luciferase reporter activities under the control of the *ICS1* promoter in *N. benthamiana* leaves transiently expressing NTL9, $NTL9_{1–330}$, or the empty vector control. Representative images are shown. (*E*) ChIP experiments were performed using the CHE_{OE} plants. The long horizontal line represents the *ICS1* promoter. The short horizontal lines (lines a, b, and c) show the regions where different quantitative PCR (qPCR) primers amplify. The tick above the line represents the TCP-binding site (TBS) in region c. Error bars represent SE ($n = 3$).

expressing a β-glucuronidase reporter driven by the *NTL9* promoter, Yoon et al. have also confirmed that *NTL9* is preferentially expressed in guard cells (35). The NTL9 protein contains a NAC (petunia NAM and *Arabidopsis* ATAF1, ATAF2, and CUC2) family DNA-binding domain in the N-terminal region and a transmembrane motif in the C-terminal region (Fig. S3*A*) (35). Full-length NTL9 was reported to localize in the endoplasmic reticulum whereas the N-terminal fragment ($NTL9_{1–330}$) without the transmembrane motif was localized to the nucleus (Fig. S3 *B* and *C*) (35, 37). Overexpression of $NTL9_{1–330}$ leads to up-regulation of senescence-associated genes, suggesting that $NTL9_{1–330}$ is transcriptionally active (35, 37). To test whether NTL9 could activate the promoter of *ICS1* in planta, NTL9 or $NTL9_{1–330}$ was transiently expressed in *Nicotiana benthamiana* together with a luciferase reporter gene driven by the *ICS1* promoter. A luciferase assay showed that the full-length NTL9 only slightly activated the expression of luciferase (Fig. 1*C*), which could be explained by the fact that NTL9 was mostly

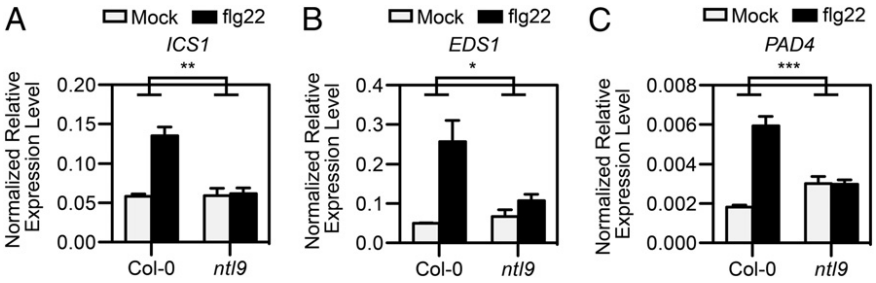

Fig. 2. NTL9 is responsible for the flg22-triggered induction of *ICS1* (*A*), *EDS1* (*B*), and *PAD4* (*C*) in guard cells. Leaves were treated with either the mock solution or 5 μM flg22 for 1 h before being used for guard cell isolation. Transcription inhibitors were added during the isolation procedure. The relative expression levels were calculated using the constitutively expressed *ACT2* as a control. Error bars represent SE of three biological replicates. Two-way ANOVA was used to test the statistical significance of the interaction. Col-0, WT. $*P < 0.05$; $**P < 0.01$; $***P < 0.001$.

observed outside the nucleus (Fig. S3*B*). In contrast, $NTL9_{1–330}$ strongly activated luciferase expression (Fig. 1*C*), demonstrating that the DNA-binding domain of NTL9 can bind to the promoter of *ICS1* not only in yeast but also in planta. In addition to *ICS1,* NTL9 also interacted with the promoters of *EDS1, PAD4*, and *PBS3* (Fig. 1*B*), suggesting that NTL9 may coordinately regulate these four SA synthesis-related genes.

As a TCP family TF, our second candidate TF CHE has been shown to bind to the class I TCP-binding site (TBS) (25). We found that the *ICS1* promoter contains one such TBS and that mutations introduced to this site completely abolished CHE binding to the *ICS1* promoter in yeast (Fig. 1*D*). This binding was further demonstrated in planta using chromatin immunoprecipitation (ChIP) performed in a *35S:CHE-GFP* transgenic line overexpressing CHE (CHE_{OE}) (Fig. 1*E*). However, unlike NTL9, CHE could not interact with promoters of *EDS1, PAD4*, and *PBS3* (Fig. 1*F*), consistent with the fact that these promoters do not contain the CHE-binding *cis*-element and that they are not expressed in-phase with either *ICS1* or *CHE* based on the publicly available microarray data (33).

Our yeast one-hybrid screen and the subsequent analyses identified NTL9 and CHE as viable candidate TFs in regulating *ICS1* expression and SA biosynthesis. Their expression patterns suggest distinct immune responses in which their roles should be tested.

NTL9 Is Required for the Flagellin-Triggered Induction of SA Synthesis-Related Genes in Guard Cells. Because exogenous application of SA can trigger stomatal closure, it is reasonable to extrapolate that an increase in the expression of SA synthesis-related genes and the endogenous SA levels in guard cells might be the signaling event between flagellin perception and stomatal closure. To test this hypothesis, guard cells were isolated from the WT plant and the *ntl9* mutant (SALK_065051) 1 h after treatment with flg22 (the 22-amino acid epitope in flagellin). Transcription inhibitors were added during guard cell isolation to avoid transcriptional changes caused by the isolation procedure. As shown in Fig. 2 *A, B*, and *C*, the expression of *ICS1*, *EDS1*, and *PAD4* was induced by flg22 in WT guard cells whereas the expression level of *PBS3* was too low for accurate detection. However, in the *ntl9* mutant, flg22-mediated induction of *ICS1*, *EDS1*, and *PAD4* was compromised. These results demonstrated that SA synthesis-related genes *ICS1*, *EDS1*, and *PAD4* are rapidly induced in guard cells by flg22 and that this response is mediated by NTL9.

NTL9 Is a Distinct Transcription Activator Required for flg22-Triggered Stomatal Immunity. We next examined a possible role of NTL9 in stomatal immunity. We found that, similar to the previously reported *Pseudomonas syringae* pv. *tomato* DC3000 (12), *Psm* ES4326 could also decrease the average stomatal aperture in WT plants after 1 h of surface exposure (Fig. 3*A*). However, the same treatment did not change the average stomatal aperture in either the flagellin receptor mutant *fls2* or the *ntl9* mutant (Fig. 3*A*). To determine whether NTL9 is required for the flagellin-induced stomatal closure, the flg22 peptide was used instead of the bacterial pathogen. We found that the flg22-induced stomatal closure was similarly abolished in the *ntl9* mutant (Fig. 3*B*). This phenotype was rescued by expressing *NTL9-YFP* in the *ntl9* mutant background (*35S:NTL9-YFP/ntl9*) (Fig. S4), confirming the role of NTL9 in stomatal immunity.

We then examined the responsiveness of the *ntl9* mutant to exogenous application of SA. In support of our hypothesis that NTL9 is a transcription activator of SA synthesis in guard cells, the stomatal phenotype of *ntl9* was rescued by the SA treatment (Fig. 3*C*). Moreover, the defect in the *ntl9* mutant seemed to be specific to pathogen signals (e.g., flg22) because it was fully responsive to the drought stress hormone abscisic acid (ABA) (Fig. 3*D*).

In addition to *NTL9*, which is preferentially expressed in guard cells, other SA biosynthesis TF genes, *CHE*, *SARD1*, and *CBP60g,* all have detectable basal expression in guard cells and may also be involved in the flg22-triggered stomatal closure. We tested this possibility by examining the stomatal response in the *che-2* and *cbp60g* single mutants and the *cbp60g sard1* double mutant. We excluded the *sard1* single mutant because the flg22-mediated induction of the WT *SARD1* occurs later than the stomatal response (12, 21). Regardless, none of these mutants tested showed a defect in stomatal response to the flg22 treatment in contrast to *ntl9* and the receptor mutant *fls2* (Fig. 3*B*), indicating that NTL9 is the only TF currently identified that positively regulates *ICS1* expression during stomatal immunity.

We further investigated the stomatal immune response in the *ntl9* mutant by surface-inoculating *Psm* ES4326. As shown in Fig. 3 *E* and *F*, compared with the WT plants, the *ntl9* mutant displayed more disease symptoms (chlorosis and necrosis) 3 d postinoculation (dpi), similar to the flagellin receptor mutant *fls2*. Correlating with the symptoms, bacterial titers inside the leaves were significantly higher in both the *ntl9* mutant and the *fls2* mutant than bacterial titers found in WT plants. In contrast, when *Psm* ES4326 was pressure-infiltrated into the leaf apoplast, bypassing stomata, no consistent differences in bacterial titers between WT plants and the *ntl9* mutant were observed. Based on these results, we conclude that NTL9 is specifically required for SA synthesis in guard cells and plays an essential role in the flg22-triggered stomatal immunity.

CHE Is Required for the Circadian Oscillation of the *ICS1* Transcript and SA Levels. In parallel to our study of NTL9, we characterized the second TF identified in our screen, CHE, for its possible role in the circadian oscillation of *ICS1*. We first confirmed that *CHE* and *ICS1* were expressed in phase under constant light conditions (Fig. 4 *A* and *B*). We found that the oscillation of the *ICS1*

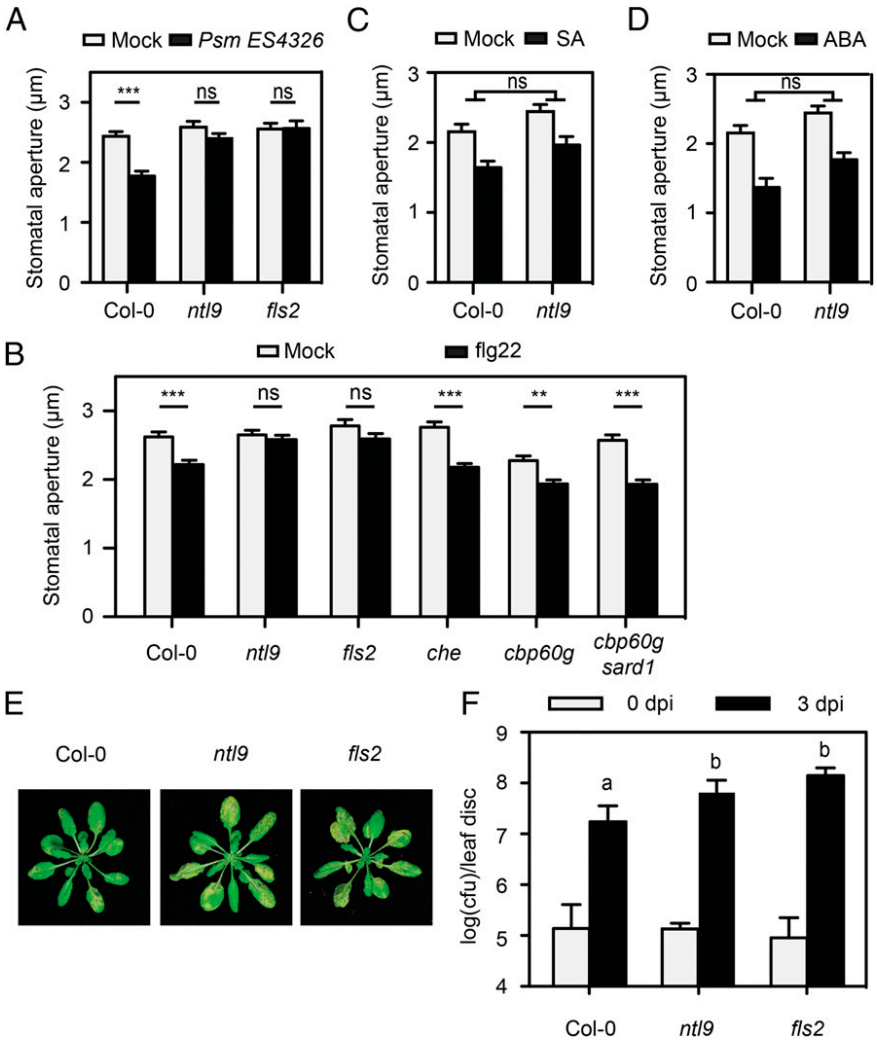

Fig. 3. NTL9 is required for flg22-triggered stomatal closure and stomatal immunity. (*A–D*) Stomatal aperture was measured 1 h after incubation with (*A*) *Psm* ES4326 (OD_{600nm} = 0.2) or (*B*) 5 μM flg22, and after 2 h incubation with either (*C*) 20 μM SA or (*D*) 10 μM ABA. Error bars represent SE of results from at least 70 stomata. One-way ANOVA was used to analyze statistical significance in *A* and *B*. For *C* and *D*, statistical significance of interaction was analyzed by two-way ANOVA. $^{**}P < 0.01$; $^{***}P < 0.001$. ns, not significant. (*E* and *F*) Plants were dip-inoculated with *Psm* ES4326 (OD_{600nm} = 0.2). (*E*) Photographs were taken of the infected plants 3 d postinoculation (dpi). (*F*) Bacterial growth was measured at the same time as in *E*. Error bars represent 95% confidence intervals (n = 8). Bonferroni's multiple comparison test was performed to compare the log-transformed data. *P* value cutoff was 0.01. Means with the same letter are not significantly different from each other. The bacterial titer on 0 dpi was not significantly different among all three genotypes.

transcript was significantly dampened in the *che-2* mutant (SAIL_1284_G12) (Fig. 4*A*), demonstrating that CHE is responsible for the circadian expression rhythm of *ICS1*. Consistently, circadian oscillations of both SA and its storage form, SA glucoside (SAG), were diminished in the *che-2* mutant plants under constant light conditions (Fig. 4 *C* and *D*).

CHE Regulates Systemic Induction of *ICS1* and SA Biosynthesis upon Pathogen Challenge. To determine whether CHE plays a role in defense response, we further tested the expression of *ICS1* in response to SA treatment in two *che* mutant alleles, *che-1* (SALK_143403) and *che-2*. Interestingly, the induction of *ICS1* by SA was clearly blocked in these *che* mutants (Fig. 5*A*). This SA-mediated induction of its own synthesis gene has been hypothesized to play a role in amplifying the SA signal for the establishment of SAR (27, 38). Therefore, the effect of the *che* mutation on pathogen-triggered systemic induction of *ICS1* was subsequently examined. *Psm* ES4326 carrying the pathogen effector *avrRpt2* was infiltrated locally (leaf 3 and 4), and gene expression in both local (leaf 3 and 4) and systemic tissues (leaf 5 and 6) was analyzed, respectively. The result showed that, whereas the local induction of *ICS1* was not dramatically affected in *che-2* (Fig. 5*B*), the systemic induction of *ICS1* was almost completely blocked in this mutant (Fig. 5*C*). Collectively, these data demonstrated that CHE is a positive regulator of *ICS1* for its circadian expression as well as its systemic induction during SAR.

The compromised expression of *ICS1* in the *che-2* mutant led us to further examine other SAR-related phenotypes in this mutant. As shown in Fig. 5 *D* and *E*, both SA and SAG levels in systemic tissues were lower in the *che-2* mutant than those in WT plants in response to *Psm* ES4326/*avrRpt2* challenge. Consistently, the expression of *PR1* gene, a widely used marker for SA-mediated response, was compromised in the *che-2* mutant (Fig. 5*F*). These results revealed that CHE is essential for inducing SA synthesis in systemic tissues during SAR.

Subsequently, the systemic resistance response was tested in WT, *che-2*, and the SA-insensitive mutant *npr1*. As shown in Fig. 5*G* and Fig. S5, SAR against the virulent bacterial pathogen *Psm* ES4326 was completely abolished in the *che-2* mutant as in *npr1*, indicating that a functional CHE is important for the

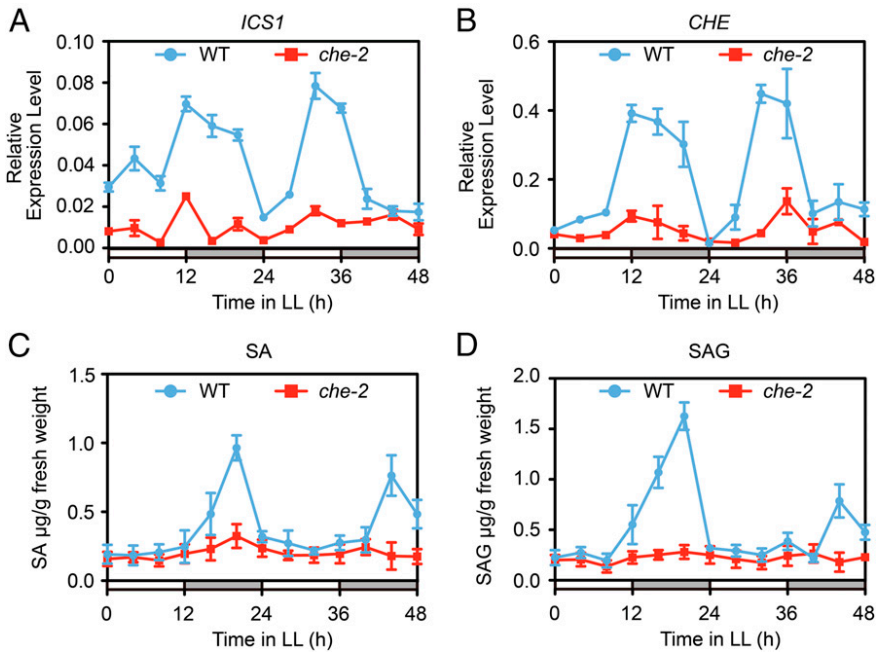

Fig. 4. CHE regulates the circadian oscillations of *ICS1* transcript and SA levels. WT plants and the *che-2* mutant previously entrained under the 12 h light/12 h dark cycles were analyzed under constant light (LL) for the *ICS1* (*A*) and *CHE* (*B*) transcript levels and SA (*C*) and SAG (*D*) levels. White bars indicate subjective days and gray bars indicate subjective nights. Error bars represent SDs of three technical replicates (*A* and *B*) or SEs of three biological replicates (*C* and *D*). Nonlinear regression analysis followed by *t* test (performed by GraphPad Prism 6) suggested that both SA and SAG have higher levels in WT than in the *che-2* mutant ($P < 0.0001$).

establishment of SAR. Interestingly, growth of *Psm* ES4326 was also slightly higher in the mock-treated *che* mutant compared with the mock-treated WT, indicating that *che* is partially compromised in basal resistance either through a defect in SA biosynthesis or an unknown mechanism.

CHE Regulates *CBP60g* and *SARD1* Expression During SAR. Besides CHE, SARD1 and CBP60g are two other positive TFs of *ICS1* during SAR. Although the activity of CBP60g requires calmodulin binding and may be modulated by Ca^{2+}, both *CBP60g* and *SARD1* are activated transcriptionally upon pathogen infection, and their upstream regulators are still unknown (18, 21, 39). We tested a possible role for CHE in systemic induction of *CBP60g* and *SARD1* genes and found the *che-2* mutation significantly diminished the induction of both genes (Fig. 6 *A* and *B*). Therefore, in addition to the direct induction of *ICS1*, CHE may also activate the transcription of *CBP60g* and *SARD1* to further induce *ICS1* in systemic tissues during SAR. Because the CHE-binding *cis*-element is not found in the promoters of *CBP60g* and *SARD1*, this activation is likely through an indirect mechanism.

Discussion

Our study of NTL9 and CHE shows that SA biosynthesis is regulated by distinct TFs in a spatial and temporal manner. Although the role of SA in stomatal immunity has been well-demonstrated (21), it was not known previously whether this response involves the basal level of SA or requires new biosynthesis. The guard cell-specific gene expression analysis performed in this study showed that some of the SA synthesis-related genes were rapidly induced by flg22 accompanied by the stomatal closure response (both occurring about 1 h after treatment). Although the observed induction of these SA synthesis genes was only two- to threefold, this induction is within the range detected in systemic tissues during SAR (18). Currently, it is difficult to measure SA levels in guard cells directly due to technical impediments.

The mechanism by which NTL9 is activated upon perception of the microbe-associated molecular pattern (MAMP) signal flg22 in guard cells requires further investigation. Because NTL9 contains a transmembrane domain, it is possible that its TF domain is released from association with the membrane through cleavage as previously proposed (35, 37). However, this mechanism needs to be further examined specifically in guard cells.

In a genome-wide interactome study, NTL9 was found to physically interact with one effector from *P. syringae* and four effectors from *Hyaloperonospora arabidopsidis* (40). These effectors might target NTL9 to facilitate infection by inhibiting immune responses, such as stomatal immunity induced by flg22. Indeed, a recent study showed that the *P. syringae* effector HopD1 interacts with NTL9 and inhibits NTL9-mediated induction of certain immune genes during effector-triggered immunity (ETI) (37). Therefore, although NTL9 expression level is low in mesophyll cells, NTL9 may also have a defense function in these cells. However, whether NTL9 is required for *ICS1* induction during ETI requires further investigation.

It is intriguing that the clock component CHE is responsible not only for the circadian expression of *ICS1* but also for the systemic induction of *ICS1* and SA accumulation during the onset of SAR. The *ICS1* promoter contains only one known *cis*-element for TCP; therefore, it is possible that CHE and other TCPs, such as TCP8 and TCP9 identified by Wang et al. (20), compete for this binding site. At the local infection site, TCP8/9 may have a stronger binding affinity to the *ICS1* promoter than CHE, whereas in the systemic tissue, CHE plays a predominant role. Moreover, CHE is specifically responsible for the rhythmic synthesis of SA during the circadian cycle.

Before this report, two other TFs (SARD1 and CBP60g) were identified to induce *ICS1* expression and SA accumulation in local defense and SAR (18, 21). Interestingly, the systemic induction of *CBP60g* and *SARD1* is partially dependent on CHE, suggesting the existence of a transcriptional amplification network for *ICS1* induction and SA accumulation in systemic tissues.

The signal that activates CHE during the onset of SAR has yet to be identified. Several mobile signals, such as methyl SA, azelaic acid, glycerol-3-phosphate, abietane diterpenoid dehydroabietinal,

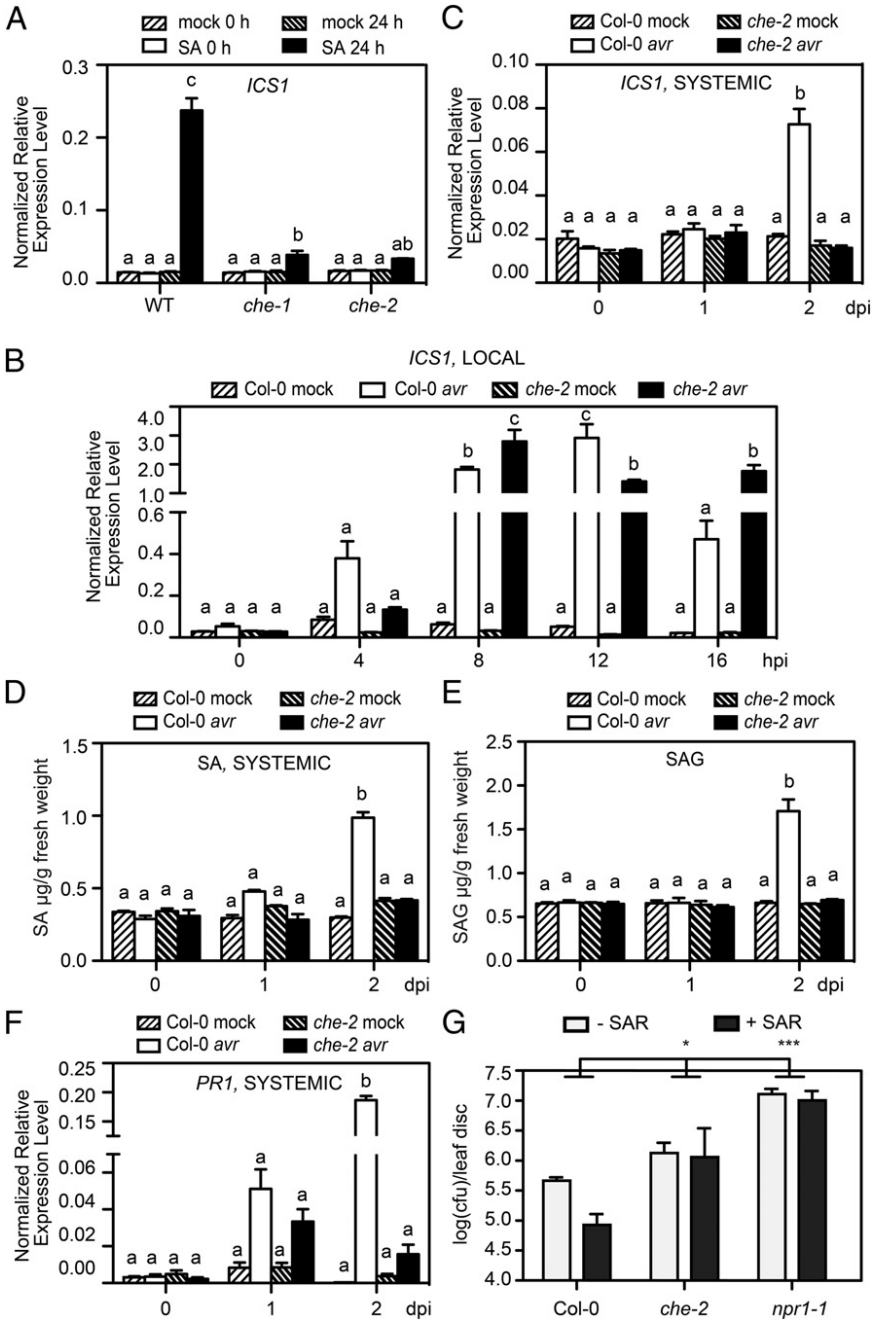

Fig. 5. CHE is required for the systemic induction of SA and establishment of SAR. (*A*) Leaves were collected at 0 h and 24 h after being sprayed with water (mock) or 1 mM SA. SA-triggered *ICS1* induction was measured by qPCR using the constitutively expressed *UBQ5* as a control. One-way ANOVA, followed by Tukey's multiple comparisons test, was used for statistical analysis ($P < 0.05$). Means with the same letter are not significantly different from each other. Error bars represent SEs from three biological replicates. (*B, C, D, E,* and *F*) Local induction of *ICS1* (*B*) and systemic induction of *ICS1* (*C*), SA level (*D*), SAG level (*E*), and *PR1* (*F*) by local inoculation of 10 mM $MgSO_4$ (mock) or *Psm* ES4326/*avrRpt2* (*avr*) ($OD_{600nm} = 0.02$). Local tissues were collected at 0, 4, 8, 12, and 16 h postinoculation (hpi). Systemic tissues were collected at 0, 1, and 2 d postinoculation (dpi). One-way ANOVA, followed by Tukey's multiple comparisons test, was used for statistical analysis ($P < 0.05$). Means with the same letter are not significantly different from each other. Error bars represent SEs from three biological replicates. (*G*) Plants were infiltrated with 10 mM $MgSO_4$ (-SAR) or *Psm* ES4326/*avrRpt2* ($OD_{600nm} = 0.02$) (+SAR). Three days later, systemic leaves were infiltrated with *Psm* ES4326 ($OD_{600nm} = 0.001$). Bacterial growth in systemic leaves was measured 3 d after the second pathogen infection. Error bars represent 95% confidence intervals ($n = 8$). Two-way ANOVA analysis was used to test statistical significance. $*P < 0.05$; $***P < 0.001$.

and pipecolic acid, have been reported to be required for inducing resistance in systemic tissues (41–45). They are possible candidate signals for enhancing CHE's activity.

Through this study, we discovered that SA biosynthesis is regulated by multiple TFs in a spatial and temporal manner. In guard cells, SA synthesis genes are transcriptionally induced within 1 h after exposure to a MAMP signal whereas systemic induction in SA production takes place 48 h after a local infection. NTL9 and CHE, together with the previously identified SARD1, CBP60g, and TCP8/9, all contribute to the induction of SA biosynthesis as a general defense response in plants against a wide range of pathogens.

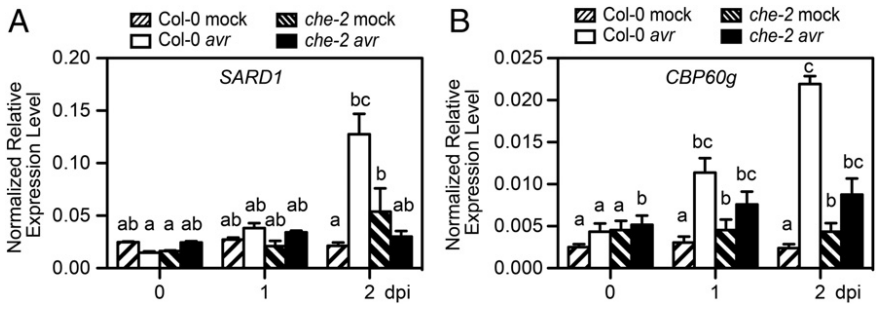

Fig. 6. CHE is required for pathogen-mediated systemic induction of *SARD1* and *CBP60g*. Plants were infiltrated with 10 mM $MgSO_4$ (mock) or *Psm* ES4326/*avrRpt2* (*avr*, OD_{600nm} = 0.02), and systemic tissues were collected at 0, 1, and 2 d postinoculation (dpi) to analyze the transcripts of *SARD1* (*A*) and *CBP60g* (*B*) using qPCR. Error bars represent SEs from three biological replications. One-way ANOVA, followed by Tukey's multiple comparisons test, was used for statistical analysis ($P < 0.05$). Means with the same letter are not significantly different from each other.

Experimental Procedures

Plant and Bacterial Strains. The *che-1* mutant (SALK_143403), *che-2* mutant (SAIL_1284_G12), and *CHEox* (*35S:CHE-GFP* no. 98) plants were previously described (25). The *ntl9* mutant (SALK_065051C) was obtained from the *Arabidopsis* Biological Resource Center. The coding sequence of *NTL9* was cloned to the vector pEG104 (46) to generate *35S:NTL9-YFP,* which was transformed to the *ntl9* mutant background to generate the complementation line (*35S:NTL9-YFP/ntl9*). Plants were grown in soil under 12 h light/12 h dark at about 60% humidity for 3 wk. *Psm* ES4326 and *Psm* ES4326/*avrRpt2* were grown on King's medium B (KB) plates with corresponding antibiotics at 28 °C for 2 d before plant inoculation (47, 48).

Yeast One-Hybrid Assay. Y1H screens were performed as previously described (25). The promoters of *ICS1* (1,979 bp upstream of the transcription start site), *PBS3* (2,255 bp), *EDS1* (899 bp), and *PAD4* (1,596 bp) were cloned into the pMW3 plasmid and integrated into the yeast strain YM4271 (MATa) as previously described (49). Mutagenesis of the *ICS1* promoter was performed using the QuikChange Lighting Multi Site-Directed Mutagenesis Kit (Agilent Technologies) according to the manual. *ICS1p_TBSm* (TBS mutated in the *ICS1* promoter; GTGGGCCC to TGTTTAAA) were cloned into the destination vectors pMW2 and pMW3 using the Gateway cloning kit (Invitrogen). The TFs (NTL9 and CHE) were fused with the Gal4 activation domain using pDEST22 and transformed into a MATα yeast strain. The yeast strain carrying the bait promoter was mated with the yeast strain containing either the TF-pDEST22 or the empty vector. An ortho-nitrophenyl-β-galactoside (ONPG) assay was performed similarly as previously described (25) and detailed in *SI Experimental Procedures*.

Chromatin Immunoprecipitation. A ChIP experiment was performed as previously described (16). Three-week-old Col WT and *CHEox* (*35S:CHE-GFP* no. 98) plants were used. Primers used for ChIP are listed in *SI Experimental Procedures*. Experiments were repeated three times with similar results.

Flg22 Treatment and Guard Cell Purification for Transcript Analysis. For each sample, around 70 fully expanded young leaves were taken from 4- to 5-wk-old plants. The leaves were submerged in 100 mL of the Mes buffer (10 mM KCl, 25 mM Mes-KOH, pH 6.15) containing 0.02% silwet-L77, with or without 5 μM flg22 and incubated in the original growth chamber for 1 h. Treatment always started 3 h after the lights in the chamber were on. After treatment, guard cell protoplasts were isolated similarly as previously described (50–52). The detailed protocol can be found in *SI Experimental Procedures*. Experiments were repeated three times with similar results.

RNA Extraction and Quantitative PCR. RNA was extracted using TRIzol (Ambion) as previously described (53). cDNA was synthesized using SuperScript III reverse transcriptase (Invitrogen). qPCR (quantitative PCR) using gene-specific primers was performed using SYBR Green (Roche) on the real-time PCR machine Mastercycler realplex2 (Eppendorf). *ACT2* or *UBQ5* was used as an internal control in analyzing the qPCR data for guard cells and whole leaves, respectively. The qPCR primers are listed in *SI Experimental Procedures*. Experiments were repeated three times with similar results.

SA and SAG Extraction and Measurement. As previously described (16), SA was extracted from ~200 mg of leaf tissues using 90% (vol/vol) methanol followed by 100% methanol. The samples were then vacuum-dried and suspended in 5% (vol/vol) trichloroacetic acid. SA was then extracted twice using ethyl acetate-cyclopentane (1:1 in volume). The extracts were further dried and dissolved in HPLC eluent [10% (vol/vol) methanol in 0.2 M acetate buffer] and subjected to HPLC. SAG was converted to SA by HCl at 80 °C for 1 h and then extracted and measured using the same method as for SA. Three biological replicates were taken for each data point. Experiments were repeated three times with similar results.

Stomatal Assay. The stomatal assay was performed as described previously (54). Treatments all started 3 h after the lights in the chamber were on. For *Psm* ES4326 induction, freshly grown bacteria were suspended in the Mes buffer (10 mM KCl, 25 mM Mes-KOH, pH 6.15) to a final OD_{600nm} of 0.2. For flg22, ABA, and SA treatments, stock solutions were freshly diluted in the Mes buffer for a final concentration of 5 μM flg22, 10 μM ABA, and 20 μM SA. The incubation time for *Psm* ES4326 and flg22 was 1 h; for ABA and SA, the incubation time was 2 h. Experiments were repeated three times with similar results.

***P. syringae* Dip-Inoculation Infection.** *Psm* ES4326 was grown on KB plates with 100 μM streptomycin at 28 °C for 2 d and then used to inoculate a liquid preculture (47, 48). After incubation at 28 °C for 6–8 h, the preculture was used to inoculate the final liquid culture in 1:500 dilution and incubated at 28 °C overnight until OD_{600nm} reached 0.8–1. The bacteria were then collected by centrifugation and suspended in 10 mM $MgCl_2$ solution with 0.02% Silwet L-77 to OD_{600nm} of 0.2. Plants were grown in mesh-covered pots. In early morning, 4-wk-old plants were dipped into the prepared *Psm* ES4326 suspension. After the liquid on the leaf surface dried out, the plants were put into a growth chamber with 90% humidity and covered with a clear plastic lid until lights were turned off on that day. The lid was removed for the rest of the experiment. Three days after inoculation, from each plant the same four leaves (leaf 8–leaf 11) were taken as one single sample. Eight samples (from eight plants) were collected as biological replicates in each experiment. The infected leaves were surface-sterilized with 75% (vol/vol) ethanol and washed twice. Then the leaves were homogenized to assay the bacterial growth as described previously (55). The 0 dpi samples were not surface-sterilized. Statistical analyses were performed on means of log-transformed data using one-way ANOVA and Bonferroni's multiple comparison tests (*P* value cutoff was 0.001). Experiments were repeated three times with similar results.

SAR Assay. A SAR assay was performed as previously described (56). Briefly, leaf 3 and leaf 4 of 3-wk-old plants were pressure-infiltrated with 10 mM $MgSO_4$ (mock treatment) or avirulent bacterial pathogen *Psm* ES4326 carrying *avrRpt2* (OD_{600nm} = 0.02). Three days later, virulent bacterial pathogen *Psm* ES4326 (OD_{600nm} = 0.001) was infiltrated into leaf 5 and leaf 6 (systemic leaves). Eight plants/genotype/treatment were used. Sampling was performed 3 d post inoculation to analyze the bacterial growth. Experiments were repeated three times with similar results.

ACKNOWLEDGMENTS. We thank Dr. Jane Glazebrook for providing the *cbp60g* single mutant and the *cbp60g sard1* double mutant, Dr. Weiqing Zeng for advice on the stomatal assay, Dr. Zhen-Ming Pei for advice on guard cell protoplast isolation, Dr. Wei Wang for help in collecting time-course samples and statistical analysis, and Dr. Yangnan Gu for assisting with the confocal imaging. This study was supported by National Science Foundation Grant IOS 0929226 and NIH Grant 1R01-GM099839-01 and by Howard Hughes Medical

Institute-Gordon and Betty Moore Foundation Grant GBMF3032 (to X.D.); by NIH-National Institute of General Medical Sciences Grants R01GM056006, R01GM067837, and RC2GM092412 (to S.A.K.) and R01GM056006 (to J.L.P-P.) as coinvestigator; and by a Hargitt Fellowship (to H.Y.).

1. Vlot AC, Dempsey DA, Klessig DF (2009) Salicylic Acid, a multifaceted hormone to combat disease. *Annu Rev Phytopathol* 47:177–206.
2. Durrant WE, Dong X (2004) Systemic acquired resistance. *Annu Rev Phytopathol* 42: 185–209.
3. Malamy J, Carr JP, Klessig DF, Raskin I (1990) Salicylic Acid: A likely endogenous signal in the resistance response of tobacco to viral infection. *Science* 250(4983):1002–1004.
4. Métraux JP, et al. (1990) Increase in salicylic acid at the onset of systemic acquired resistance in cucumber. *Science* 250(4983):1004–1006.
5. White RF (1979) Acetylsalicylic acid (aspirin) induces resistance to tobacco mosaic virus in tobacco. *Virology* 99(2):410–412.
6. Gaffney T, et al. (1993) Requirement of salicylic acid for the induction of systemic acquired resistance. *Science* 261(5122):754–756.
7. Nawrath C, Métraux JP (1999) Salicylic acid induction-deficient mutants of Arabidopsis express PR-2 and PR-5 and accumulate high levels of camalexin after pathogen inoculation. *Plant Cell* 11(8):1393–1404.
8. Halim VA, et al. (2007) Salicylic acid is important for basal defense of Solanum tuberosum against Phytophthora infestans. *Mol Plant Microbe Interact* 20(11): 1346–1352.
9. Yang Y, Qi M, Mei C (2004) Endogenous salicylic acid protects rice plants from oxidative damage caused by aging as well as biotic and abiotic stress. *Plant J* 40(6): 909–919.
10. Wang D, Weaver ND, Kesarwani M, Dong X (2005) Induction of protein secretory pathway is required for systemic acquired resistance. *Science* 308(5724):1036–1040.
11. Yalpani N, Silverman P, Wilson TM, Kleier DA, Raskin I (1991) Salicylic acid is a systemic signal and an inducer of pathogenesis-related proteins in virus-infected tobacco. *Plant Cell* 3(8):809–818.
12. Melotto M, Underwood W, Koczan J, Nomura K, He SY (2006) Plant stomata function in innate immunity against bacterial invasion. *Cell* 126(5):969–980.
13. Zeng W, He SY (2010) A prominent role of the flagellin receptor FLAGELLIN-SENSING2 in mediating stomatal response to Pseudomonas syringae pv tomato DC3000 in Arabidopsis. *Plant Physiol* 153(3):1188–1198.
14. Wildermuth MC, Dewdney J, Wu G, Ausubel FM (2001) Isochorismate synthase is required to synthesize salicylic acid for plant defence. *Nature* 414(6863):562–565.
15. Strawn MA, et al. (2007) Arabidopsis isochorismate synthase functional in pathogen-induced salicylate biosynthesis exhibits properties consistent with a role in diverse stress responses. *J Biol Chem* 282(8):5919–5933.
16. Zheng XY, et al. (2012) Coronatine promotes Pseudomonas syringae virulence in plants by activating a signaling cascade that inhibits salicylic acid accumulation. *Cell Host Microbe* 11(6):587–596.
17. Chen H, et al. (2009) ETHYLENE INSENSITIVE3 and ETHYLENE INSENSITIVE3-LIKE1 repress SALICYLIC ACID INDUCTION DEFICIENT2 expression to negatively regulate plant innate immunity in Arabidopsis. *Plant Cell* 21(8):2527–2540.
18. Zhang Y, et al. (2010) Control of salicylic acid synthesis and systemic acquired resistance by two members of a plant-specific family of transcription factors. *Proc Natl Acad Sci USA* 107(42):18220–18225.
19. van Verk MC, Bol JF, Linthorst HJ (2011) WRKY transcription factors involved in activation of SA biosynthesis genes. *BMC Plant Biol* 11:89.
20. Wang X, et al. (2015) TCP transcription factors are critical for the coordinated regulation of isochorismate synthase 1 expression in Arabidopsis thaliana. *Plant J* 82(1): 151–162.
21. Wang L, et al. (2011) CBP60g and SARD1 play partially redundant critical roles in salicylic acid signaling. *Plant J* 67(6):1029–1041.
22. Goodspeed D, Chehab EW, Min-Venditti A, Braam J, Covington MF (2012) Arabidopsis synchronizes jasmonate-mediated defense with insect circadian behavior. *Proc Natl Acad Sci USA* 109(12):4674–4677.
23. Wang W, et al. (2011) Timing of plant immune responses by a central circadian regulator. *Nature* 470(7332):110–114.
24. Kim SY, et al. (2007) Exploring membrane-associated NAC transcription factors in Arabidopsis: Implications for membrane biology in genome regulation. *Nucleic Acids Res* 35(1):203–213.
25. Pruneda-Paz JL, Breton G, Para A, Kay SA (2009) A functional genomics approach reveals CHE as a component of the Arabidopsis circadian clock. *Science* 323(5920): 1481–1485.
26. Li L, et al. (2012) Linking photoreceptor excitation to changes in plant architecture. *Genes Dev* 26(8):785–790.
27. Zhou N, Tootle TL, Tsui F, Klessig DF, Glazebrook J (1998) PAD4 functions upstream from salicylic acid to control defense responses in Arabidopsis. *Plant Cell* 10(6): 1021–1030.
28. Feys BJ, Moisan LJ, Newman MA, Parker JE (2001) Direct interaction between the Arabidopsis disease resistance signaling proteins, EDS1 and PAD4. *EMBO J* 20(19): 5400–5411.
29. Nobuta K, et al. (2007) The GH3 acyl adenylase family member PBS3 regulates salicylic acid-dependent defense responses in Arabidopsis. *Plant Physiol* 144(2):1144–1156.
30. Hruz T, et al. (2008) Genevestigator v3: A reference expression database for the meta-analysis of transcriptomes. *Adv Bioinforma* 2008:420747.
31. Winter D, et al. (2007) An "Electronic Fluorescent Pictograph" browser for exploring and analyzing large-scale biological data sets. *PLoS ONE* 2(8):e718.
32. Yang Y, Costa A, Leonhardt N, Siegel RS, Schroeder JI (2008) Isolation of a strong Arabidopsis guard cell promoter and its potential as a research tool. *Plant Methods* 4:6.
33. Mockler TC, et al. (2007) The DIURNAL project: DIURNAL and circadian expression profiling, model-based pattern matching, and promoter analysis. *Cold Spring Harb Symp Quant Biol* 72:353–363.
34. Kim HS, et al. (2007) Identification of a calmodulin-binding NAC protein as a transcriptional repressor in Arabidopsis. *J Biol Chem* 282(50):36292–36302.
35. Yoon HK, Kim SG, Kim SY, Park CM (2008) Regulation of leaf senescence by NTL9-mediated osmotic stress signaling in Arabidopsis. *Mol Cells* 25(3):438–445.
36. Kim HS, et al. (2012) A NAC transcription factor and SNI1 cooperatively suppress basal pathogen resistance in Arabidopsis thaliana. *Nucleic Acids Res* 40(18):9182–9192.
37. Block A, et al. (2014) The Pseudomonas syringae type III effector HopD1 suppresses effector-triggered immunity, localizes to the endoplasmic reticulum, and targets the Arabidopsis transcription factor NTL9. *New Phytol* 201(4):1358–1370.
38. Jirage D, et al. (1999) Arabidopsis thaliana PAD4 encodes a lipase-like gene that is important for salicylic acid signaling. *Proc Natl Acad Sci USA* 96(23):13583–13588.
39. Wang L, et al. (2009) Arabidopsis CaM binding protein CBP60g contributes to MAMP-induced SA accumulation and is involved in disease resistance against Pseudomonas syringae. *PLoS Pathog* 5(2):e1000301.
40. Mukhtar MS, et al.; European Union Effectoromics Consortium (2011) Independently evolved virulence effectors converge onto hubs in a plant immune system network. *Science* 333(6042):596–601.
41. Park SW, Kaimoyo E, Kumar D, Mosher S, Klessig DF (2007) Methyl salicylate is a critical mobile signal for plant systemic acquired resistance. *Science* 318(5847):113–116.
42. Maldonado AM, Doerner P, Dixon RA, Lamb CJ, Cameron RK (2002) A putative lipid transfer protein involved in systemic resistance signalling in Arabidopsis. *Nature* 419(6905):399–403.
43. Chanda B, et al. (2011) Glycerol-3-phosphate is a critical mobile inducer of systemic immunity in plants. *Nat Genet* 43(5):421–427.
44. Chaturvedi R, et al. (2012) An abietane diterpenoid is a potent activator of systemic acquired resistance. *Plant J* 71(1):161–172.
45. Návarová H, Bernsdorff F, Döring AC, Zeier J (2012) Pipecolic acid, an endogenous mediator of defense amplification and priming, is a critical regulator of inducible plant immunity. *Plant Cell* 24(12):5123–5141.
46. Earley KW, et al. (2006) Gateway-compatible vectors for plant functional genomics and proteomics. *Plant J* 45(4):616–629.
47. Dong X, Mindrinos M, Davis KR, Ausubel FM (1991) Induction of Arabidopsis defense genes by virulent and avirulent Pseudomonas syringae strains and by a cloned avirulence gene. *Plant Cell* 3(1):61–72.
48. Cui J, et al. (2005) Pseudomonas syringae manipulates systemic plant defenses against pathogens and herbivores. *Proc Natl Acad Sci USA* 102(5):1791–1796.
49. Deplancke B, Vermeirssen V, Arda HE, Martinez NJ, Walhout AJM (2006) Gateway-compatible yeast one-hybrid screens. *CSH Protocols*, 10.1101/pdb.prot4590.
50. Leonhardt N, et al. (2004) Microarray expression analyses of Arabidopsis guard cells and isolation of a recessive abscisic acid hypersensitive protein phosphatase 2C mutant. *Plant Cell* 16(3):596–615.
51. Obulareddy N, Panchal S, Melotto M (2013) Guard cell purification and RNA isolation suitable for high-throughput transcriptional analysis of cell-type responses to biotic stresses. *Mol Plant Microbe Interact* 26(8):844–849.
52. Pandey S, Wang XQ, Coursol SA, Assmann SM (2002) Preparation and applications of Arabidopsis thaliana guard cell protoplasts. *New Phytol* 153(3):517–526.
53. Tada Y, et al. (2008) Plant immunity requires conformational changes [corrected] of NPR1 via S-nitrosylation and thioredoxins. *Science* 321(5891):952–956, and erratum (2009)325:1072.
54. Chitrakar R, Melotto M (2010) Assessing stomatal response to live bacterial cells using whole leaf imaging. *J Vis Exp* 2010(44):e2185.
55. Durrant WE, Wang S, Dong X (2007) Arabidopsis SNI1 and RAD51D regulate both gene transcription and DNA recombination during the defense response. *Proc Natl Acad Sci USA* 104(10):4223–4227.
56. Fu ZQ, et al. (2012) NPR3 and NPR4 are receptors for the immune signal salicylic acid in plants. *Nature* 486(7402):228–232.
57. Pruneda-Paz JL, et al. (2014) A genome-scale resource for the functional characterization of Arabidopsis transcription factors. *Cell Reports* 8(2):622–632.

Supporting Information

Zheng et al. 10.1073/pnas.1511182112

SI Experimental Procedures

Yeast One-Hybrid Assay. The promoters of *ICS1* (1,979 bp upstream of the transcription start site), *PBS3* (2,255 bp), *EDS1* (899 bp), and *PAD4* (1,596 bp) were cloned into the pMW3 plasmid and integrated into the yeast strain YM4271 (MATa) as previously described (49). The TFs were fused with the Gal4 activation domain using pDEST22 and transformed into the MATα yeast strain YU (57). The yeast strain carrying the promoter bait was mated with the yeast strain containing either the TF-pDEST22 or the empty vector. Diploid colonies were grown in the selective liquid medium overnight and then used to inoculate YPD liquid culture and incubated at 30 °C until OD_{600nm} reached 0.6~0.8. The accurate OD_{600nm} of each culture was measured, and three aliquots of the same volume (1 mL) were taken and used for the ONPG (ortho-Nitrophenyl-β-galactoside) assay, which was conducted similarly to previously described (25). The yeast cells were collected, suspended in 150 μL of Z Buffer (60 mM Na_2HPO_4, 40 mM NaH_2PO_4, 10 mM KCl, and 1 mM $MgSO_4$, pH 7.0) and then broken by two freeze (liquid N_2)-and-thaw cycles. Then, 850 μL of Z Buffer with 600 μg of ONPG was then added and incubated at 30 °C for 10–24 h before 400 μL of 1 M Na_2CO_3 was added to stop the reaction. The reaction was then centrifuged, and the OD_{420nm} of the supernatant was measured. The β-galactosidase activity unit was calculated by the following formula: $(OD_{420nm} \times 1000)/(OD_{600nm} \times$ reaction time $\times$ volume of cells).

Confocal Microscopic Imaging. Full-length NTL9 was tagged by YFP through cloning into the binary vector pEG104 (46), and $NTL9_{1–330}$ was tagged by CFP through cloning into the binary vector pEG102 (46). Each construct in *Agrobacterium* was infiltrated into *N. benthamiana*, and the proteins were visualized 24 h later using a Zeiss LSM 510 inverted confocal microscope.

Transient Luciferase Expression Assay. The promoter of *ICS1* was fused to the luciferase gene and was delivered by *Agrobacterium* into *N. benthamiana* with either the full-length NTL9 or $NTL9_{1–330}$ construct described above by coinfiltration. After 24–48 h, the infiltrated *N. benthamiana* leaves were rubbed with 2.5 mM luciferin (Gold Biotechnology) in 0.02% Triton X-100 (Sigma) and placed on MS plates. The leaves were then imaged using the Bio-Rad Gel Doc system.

Guard Cell Protoplast Purification. For each sample, around 70 fully expanded young leaves were taken from 4- to 5-wk-old plants. The leaves were submerged in 100 mL of treatment solution and incubated in the original growth chamber for 1 h. The treatment solution was the Mes buffer (10 mM KCl, 25 mM Mes-KOH, pH 6.15) containing 0.02% silwet-L77, with or without 5 μM flg22. Treatment always started 3 h after the lights in the chamber were on.

Guard cell protoplasts were then isolated basically as previously described (50–52). Cordycepin and actinomycin D were added in the two enzymatic incubation steps to prevent digestion-related transcriptional changes. The leaves were blended in 500 mL of water in a Waring blender for 30 s and repeated three times. The blended solution was filtered through a 100-μm nylon mesh (Spectrum Laboratories), and the flow-through was discarded. The retained epidermis fragments were transferred into a 250-mL flask containing 50 mL of the Enzyme I solution: 0.7% Cellulysin, 0.01% polyvinylpyrrolidone 40, 0.25% BSA, 55% (vol/vol) basic medium, 0.01% cordycepin, 0.0033% actinomycin D, pH 5.5. The basic medium contained 0.5 mM $CaCl_2$, 0.5 mM $MgCl_2$, 5 mM Mes, pH 5.5, adjusted by 1 M Tris·HCl solution (pH 8), and the osmolarity was adjusted to 500 mmol/kg by addition of D-sorbitol. Fragments in the Enzyme I solution were incubated in the dark at 27 °C for 30–60 min on an orbital shaker and then filtered through a 100-μm nylon mesh. After washing, the remaining fragments were transferred to another 250-mL flask containing 25 mL of the Enyzme II solution: 1.5% (wt/vol) cellulase, 0.03% pectolyase, 0.25% BSA, 0.01% cordycepin, 0.0033% actinomycin D in 100% basic medium, pH 5.5. Fragments were incubated in the Enzyme II solution in the dark at 20 °C for about 1 h until most guard cells rounded up. The solution was then filtered through a 10-μm nylon mesh, washed two times with basic medium, and all flow-through was collected and centrifuged at 1,000 × g for 5 min. The supernatant was carefully discarded with around 5 mL left. Cells were carefully resuspended and centrifuged at 1,000 × g for 5 min. All of the supernatant was carefully removed, and the protoplasts were frozen in liquid N_2 before proceeding for RNA extraction. Before the final centrifugation, the protoplasts were examined in a hemocytometer chamber. All of the samples used for RNA extraction contained around 10^6 guard cell protoplasts, and the purity was above 98%.

Stomata Assay. Stomata assays were performed as described previously (54). Fully expanded young leaves from 4- to 5-wk-old plants were stained with 20 μM propidium iodide for 5 min. After rinsing in water, the main vain was cut, and the abaxial side of the leaf was put in contact with the treatment solution. The incubation was carried out in the original growth chamber. At designated time points, the leaf was quickly imaged using a Zeiss LSM510 upright confocal microscope (excitation 458 nm, emission 560–615 nm), and the stomatal aperture was measured. For each sample point, around 60–80 stomata from multiple regions in two different leaves were measured. Treatments all started 3 h after the lights in the chamber were on. For *Psm* ES4326 treatment, freshly grown bacteria were suspended in the Mes buffer (10 mM KCl, 25 mM Mes-KOH, pH 6.15) to a final OD_{600nm} of 0.2. For flg22, SA, and ABA, stock solution was freshly diluted in the Mes buffer for a final concentration of 5 μM flg22, 20 μM SA, and 10 μM ABA. The incubation time for *Psm* ES4326 and flg22 was 1 h; for SA and ABA, the incubation time was 2 h.

Primers for ChIP.

Primer name	Primer sequences
ICS1_a_F	AGAAATTCGTAGCATCCACAACACACA
ICS1_a_R	AAACTGAAACTAGACACGGTCCTCAGA
ICS1_b_F	AAGGAGCATGCGTGTAATGCCA
ICS1_b_R	CGTTTGATACGGAAGCGGTTTGCAC
ICS1_c_F	TGCACGACTAACTTTAGAAAAATGT
ICS1_c_R	AGGGGACTGATGTAGCAGGGGC

Primers for qRT-PCR.

Primer name	Primer sequences
ICS1_F	GGCAGGGAGACTTACG
ICS1_R	AGGTCCCGCATACATT
EDS5_F	GGTCTTGGCGATACAAT
EDS5_R	CAGCGAGTGCAGAGATC
PAD4_F	TTAGCCGTTGAAGCTCT
PAD4_R	ATGCATCGCAACGATCT
EDS1_F	CTGAGTTAGCCGGTGT
EDS1_R	TTTCATGTACGGCCCTG
ACT2_F	ACACTGTGCCAATCTACGAGGGTT
ACT2_R	ACAATTTCCCGCTCTGCTGTTGTG
NLT9_F	GGGATAAAGATCCGGGCTCG
NTL9_R	TTGGCCTCGGGAATAACAGTG
CHE_ F	TAATGGGTGGTGGTGGTTCTG
CHE_ R	GCAAAGCTCCAGACTTGTCC
PR1_ F	CTCATACACTCTGGTGGG
PR1_R	TTGGCACATCCGAGTC
SARD1_ F	CCTCAACCAGCCCTACGTTA
SARD1_ R	TAGTGGCTCGCAGCATATTG
UBQ5_ F	GACGCTTCATCTCGTCC
UBQ5_ R	GTAAACGTAGGTGAGTCC

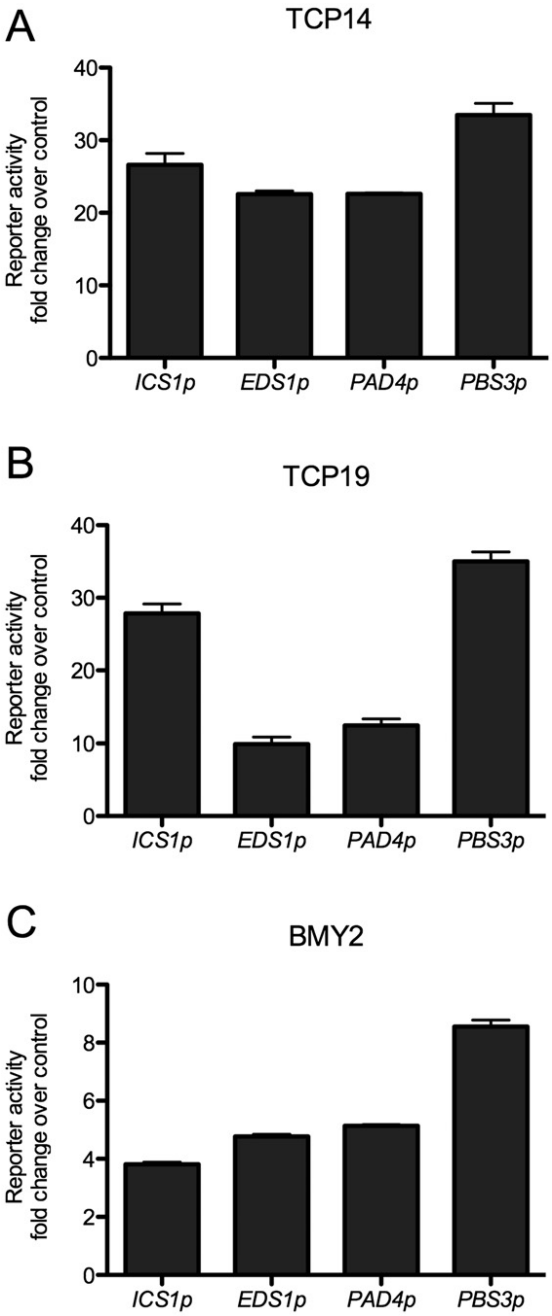

Fig. S1. TCP14, TCP19, and BMY2 interact with the promoters of *ICS1*, *EDS1*, *PAD4*, and *PBS3*. Reporter activities under the control of *ICS1*, *EDS1*, *PAD4*, or *PBS3* promoter in the presence of TCP14-AD (*A*), TCP19-AD (*B*), and BMY2-AD (*C*) are shown as fold change over the empty AD vector control without the transcription factor fusion. Error bars represent SD from three replicates.

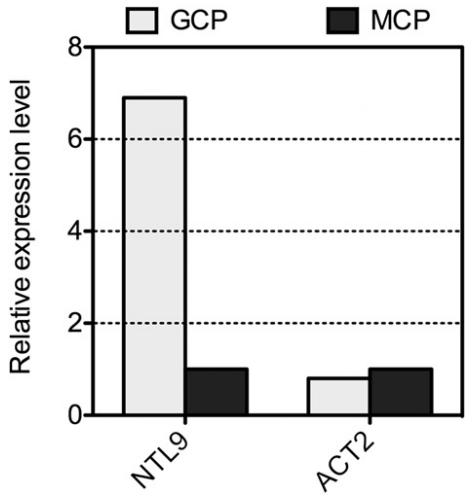

Fig. S2. *NTL9* is preferentially expressed in guard cells. Expression in guard cell protoplasts (GCPs) is presented as fold change over the expression level in mesophyll cell protoplasts (MCPs) according to the normalized microarray data (E-MEXP-1443) extracted from "The Bio-Array Resource for Plant Biology" website (bar.utoronto.ca). The constitutively expressed *ACTIN 2* gene (ACT2) was used as a control.

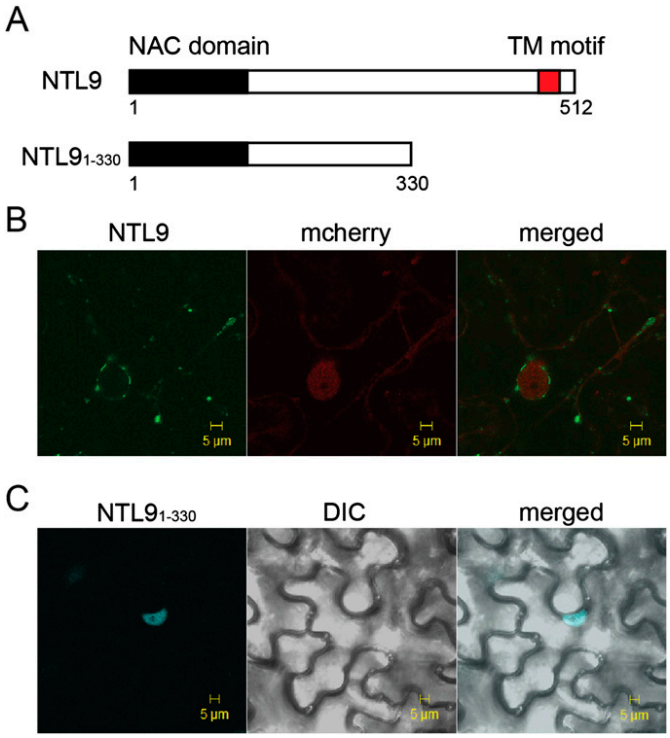

Fig. S3. NTL9 protein structure and localization. (*A*) The structure schematics of NTL9 and $NTL9_{1–330}$ are shown. NTL9-YFP and free mCherry control (*B*) or $NTL9_{1–330}$-CFP (*C*) were expressed transiently in *N. benthamiana* by *Agrobacterium* infiltration, and pictures were taken 24 h later using a Zeiss LSM 510 inverted confocal microscope.

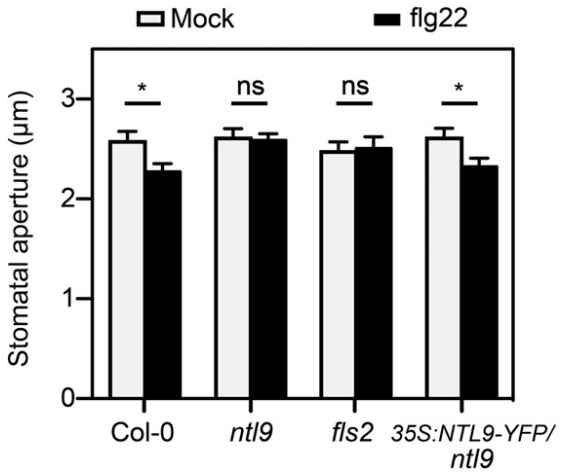

Fig. S4. The flg22-triggered stomatal closure was restored in the *ntl9* mutant by expressing *NTL9*. Stomatal apertures of WT (Col-0) plants, *ntl9, fls2*, and *35S:NTL9-YFP* in the *ntl9* background (*35S:NTL9-YFP/ntl9*) were measured 1 h after incubation with 5 μM flg22. Error bars represent SE of results from at least 40 stomata. Student's *t* test was used to analyze statistical significance. $*P < 0.05$; ns, no significant difference. Experiments were repeated three times with similar results.

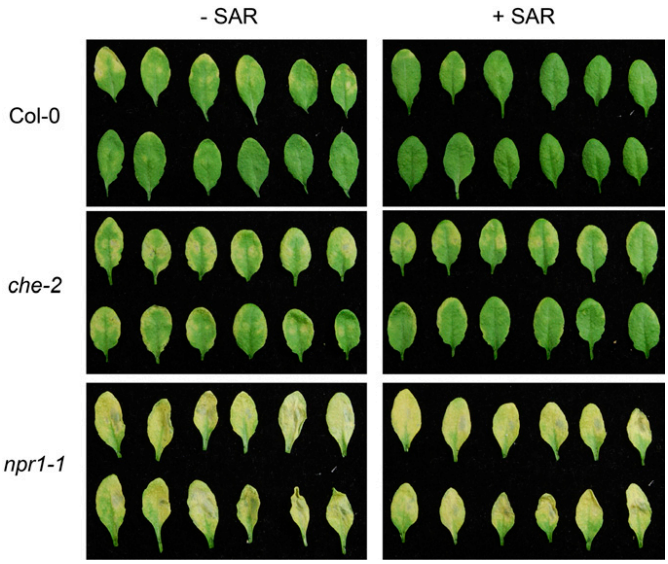

Fig. S5. Symptoms of infected systemic leaves in the SAR test showed in Fig. 5*G*. Plants were infiltrated with 10 mM $MgSO_4$ (–SAR) or *Psm* ES4326/*avrRpt2* (OD_{600nm} = 0.02) (+SAR). Three days later, systemic leaves were infiltrated with *Psm* ES4326 (OD_{600nm} = 0.001). Photographs of infected systemic leaves were taken 3 d after the second pathogen infection.

Other Supporting Information Files

Dataset S1 (XLS)
Dataset S2 (XLS)